Defect Specification Modeling Enabled Comprehensive Rating System with Individual and Collective Impact Analysis

Youheng Guo[1,2], Xuesong Shen[1], Khalegh Barati[1], and James Linke[2]

[1]School of Civil and Environmental Engineering, The University of New South Wales (UNSW Sydney), Sydney, NSW 2052, Australia
[2]GeoAI, Sydney, NSW 2019, Australia
youheng.guo@student.unsw.edu.au, x.shen@unsw.edu.au, khalegh.barati@unsw.edu.au, j.linke@geoai.au

Abstract

As the safety of civil infrastructure gains more attention nowadays, inspection plays an important role in evaluating structural conditions. Ranking the level of defect is one of the most direct ways to understand the status of the building. Traditional inspections are based on handwritten records from human inspectors, which tend to be subjective and lack consistency. Therefore, digitalizing the data is a promising solution for recording. Based on the captured data, surface defects can be visualized and parameterized. This research aims to provide an innovative framework to analyze the effect of the defects based on Defect Specification Modeling (DSM) and rank the severity of different sections. A comprehensive diagnosis is conducted by considering the type, dimension, and location of the defects. It can identify structurally dangerous areas and provide solid evidence for decision-making. A case study carried out on a cooling tower is presented to validate the proposed approach. The comparison between severity rankings based solely on defect area and a comprehensive defect index reveals the practicability of the proposed methodology.

Keywords –

Defect Specification Modeling; Defect Ranking; Decision Making

1 Introduction

Traditionally, inspections have been conducted by human inspectors. Although these inspectors possess extensive experience, the reliability of inspection records is difficult to maintain, as report quality varies between individuals, potentially causing inconsistencies within a project. Moreover, manual inspection processes are prone to introduce errors, making them inefficient and time-consuming. In recent years, advancements in Computer Vision (CV) and Light Detection and Ranging (LiDAR) technologies have facilitated the digitization of inspection records in formats such as photographs, mesh models, and point clouds. Additionally, defect Building Information Modeling (BIM) has been developed to visualize and parameterize structural defects. However, limited analysis has been conducted on these defect models. The research gap remains in effectively utilizing the generated defect BIM models to extract information for decision support and maintenance strategies. Furthermore, there are no detailed standards for assessing the impact of defects on the structural integrity of the target infrastructure.

This paper aims to utilize Digital Specification Modeling (DSM) to develop a systematic framework for leveraging the severity of existing defects while considering multiple factors defined in relevant standards. By analyzing the provided defect model, an index for different defect can be calculated, enabling the ranking of severity across different structural areas. Based on this result, maintenance strategies can be optimized for varying situations. The main contribution of this work is directing the traditional experience-based structural condition assessment to a more objective and automated process which can benefit decision-making.

2 Related Work

With the acquired defect information, conducting a thorough defect rating is essential for efficient decision-making and objective asset management over the existing structure. A well-structured rating system allows stakeholders to prioritize maintenance efforts, allocate resources effectively, and mitigate potential structural failures.

2.1 Defect Modeling in BIM

BIM is a process involving collaborating between different construction stakeholders based on a 3D model. Borrowing the concept, DSM will enable structural analysis, defect ranking, and even assisting decision making.

Borin and Cavazzini [1] recreated the Three-Dimensional (3D) shape of concrete spalling pathology in the BIM model which acts as a decision support system for the built environment. To automate the onsite data collection process and enhance the reliability of diagnosis, Dias, et al. [2] discussed the application of new inspection techniques. They applied severity of degradation to evaluate the global performance of the given façade. Bolourian [3] created a public point cloud dataset for surface defect semantic segmentation and proposed a Deep Learning (DL) approach to detect different types of concrete surface defects in point clouds. Guo, et al. [4] proposed a Convolutional Neural Network (CNN) based approach to detect minor cracks on concrete surface. By facilitating the automated crack detection method, Guo, et al. [5] proposed an innovative approach to use photogrammetry to acquire spatial information to quantify the detected crack on image. Choi, et al. [6] classified the defects as cracks, surface deterioration, displacement, and deformation. Based on the extracted information, they proposed a semiautomated visual approach to filter building condition information and used Dynamo to convert the information into BIM. Yiğit and Uysal [7] generated a Level of Detail 3 (LOD3) Digital Twin (DT) by triangulating the high-resolution images from Unmanned Aerial Vehicle (UAV). Cracks are automatically detected with the aid of DL and converted into vectors. They think the proposed method is suitable for rapid evaluation in terms of Structural Health Monitoring (SHM). Bahreini and Hammad [8] introduced the Ontology for Concrete Surface Defects (OCSD) to provide comprehensive data related to concrete surface defects, encompassing inspection, diagnosis, defect concepts, repair, rehabilitation, and replacement.

2.2 Regulations for Defect Categorizing

Among different methods, United States Army Construction Engineering Research Laboratories (USACERL) appeared to be the most comprehensive standard. Uzarski [9] added descriptions for the USACERL Condition Index. But it is still based on inspectors' experiences when it comes to predicting the condition and repairing time.

Amani, et al. [10] overviewed Component Condition Index System (CCIS) and investigated from technology, measurement, assessment function, and component maintenance. The authors stated that Condition Index (CI) is fundamental for deciding time and cost to invest in repairing or replacing existing facilities. The CI scale rates the status of health from 0 to 100 or D to A based on rating scale theory. It is believed that condition description based on visual guidance is more efficient and it would become an integral infrastructure management system. Queensland-Government [11] suggested that the type, width, location, and orientation of cracks can significantly affect the structure durability. Therefore, accurately measuring cracks is essential for monitoring purposes. The severity is classified as hairline (less than 0.1mm), minor (0.1-0.3mm), moderate (0.3-0.6mm), and severe (more than 0.6mm). According to Queensland-Government [11], the conditions of structure are categorized into five states from good, fair, poor, very poor, to unsafe. The exposure classification is defined as relatively benign, mildly aggressive, aggressive, and most aggressive. Vicroads [12] noted that if the spall is less than 25 mm in depth or 15 cm in diameter, it can be categorized as a small spall.

Although researchers have been working on detecting existing defects and creating BIM based defect models which enhance both efficiency of capturing process and consistency of the data, several gaps remain in the prior studies. Most of the current defect models are used for visualization, while limited research has been allocated to exploit the captured defect data and develop a reproducible assessment system for scoring the condition of building components. In addition, Existing regulations can provide defect classification thresholds but lack a systematic method to quantify the defect attributes and rank the defect accordingly.

Therefore, this study aims to develop a structured defect ranking framework connecting spatial defect information and a transparent scoring method. By evaluating and converting different attributes, a more objective condition assessing method can be achieved and reproduced. Furthermore, the proposed framework can facilitate optimized maintenance and decision making for infrastructure asset management.

3 Research Methodology

This severity scoring framework is developed from structural maintenance and infrastructure inspection standards. By analyzing the provided defect model, a series of defect attributes are obtained and integrated into the proposed framework. The evaluation criterion is normalized ranging from 1 to 10 (least to most severe) which is consistent with infrastructure condition index system. The scoring discipline originates from engineering judgement and widely used inspection standards. Several factors influence the assessment results, including defect type, size, location, exposure, duration of existence and shape. Variations in prioritization can lead to different outcomes, affecting the severity ranking of different structural areas.

A flowchart outlining the assessment process for individual defects is presented below (see Figure 1). Both the influence of individual defects and the combined effect of multiple factors should be considered as seen in Equation 1, where CS stands for Component Score, IDS stands for Individual Defect Score, GF stands for Group Factor, and CF stands for Combination Factor. Although detailed measurements are presented below, weight and scaling factors will need to be adjusted according to specific cases.

$$CS = \sum (IDS \times GF \times CF) \tag{1}$$

3.1 Individual Effect

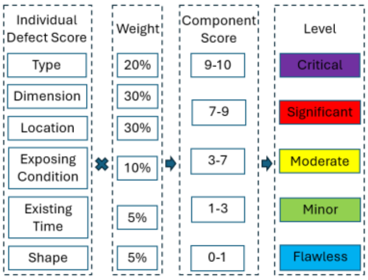

Figure 1. Proposed systematic workflow for individual defect ranking of component.

As seen in Figure 1, the component score is determined based on three key factors: defect ranking criteria, defect score (S_i), and weight (WC_i) (see Equation 2). The defect ranking criteria include defect type, dimensions, location, exposure conditions, and duration of existence. For each criterion, scores are normalized across different conditions using a ten-point scale, where a score of 10 represents the most severe extent, and a score of 1 represents the least severe level.

$$IDS = \sum_{i=1}^{n} S_i \cdot WC_i \tag{2}$$

3.1.1 Defect Type

Different types indicate different levels of potential risk. For example, cracks compromise the structural integrity of the surface, potentially leading to internal damage at early stage. While spalling typically affects a larger surface area and involves internal material exposure, it is more severe than cracking. Overall, if the defect type is more likely to pose danger to structural integrity, the severity score will correspondingly be higher.

3.1.2 Dimension

Defect dimension is one of the most direct factors that represent the level of degradation. For most defects, the affected area serves as the primary measurement criterion, while other dimensions, such as depth, width, and length, are also essential. Defects can be classified into minor, moderate, and major extents according to specific thresholds. Generally, larger defect dimensions correspond to higher severity scores.

3.1.3 Location

The location of identified defects is a significant factor influencing structural stability. Defects near critical components incur higher severity scores. The most critical areas (rated 8-10) include load-bearing components such as joints, columns, beams, and walls, where any flaw can potentially lead to structural collapse. Besides, defects at elevated locations pose significant risks, as falling debris may threaten human safety and the surrounding environment. Moderate-risk locations (rated 4-7) include slabs, floors, and ceilings. Defects in these areas may cause localized hazards but are unlikely to result in global structural failure. Non-load-bearing structures (rated 1-3), such as partition walls and cladding, are considered non-critical, as defects in these areas are less likely to cause severe structural problems.

3.1.4 Exposing Condition

Exposure conditions play a crucial role in the progression of defects. Structures fully exposed to harsh outdoor environments, such as costal erosion, high winds, severe storms, heavy snow, or intense heat, experience the highest severity levels (rated 9-10), as these extreme conditions significantly accelerate degradation and corrosion. Normal outdoor environments (rated 6-8) also have adverse effects on structural integrity, though to a lesser extent. Semi-enclosed areas, such as parking garages, patios, and sunrooms, are less affected by weather conditions and are assigned moderate severity scores (rated 3-5). Indoor environments remain relatively stable, experiencing minimal environmental impact, and therefore receive the lowest defect severity scores (rated 1-2).

3.1.5 Duration of Existence

The duration of a defect's existence is another critical factor influencing structural stability. It can be divided into three phases: emerging, developing, and existing. Developing defects (rated 8–10) are considered more significant than emerging ones, as their progression indicates increasing risk. Emerging defects (rated 4-7) may not be immediately critical. However, if a known defect is detected constantly growing, it poses a greater hazard compared to newly formed defects. In contrast, existing defects (rated 1-3) are the least concerning because they have remained stable over time without posing a major risk.

3.1.6 Shape

Moreover, the shape of a defect plays a crucial role in surface integrity. For instance, in the case of spalling, the characteristics of its edges can vary. Defects with spiky or sharp edges (rated 6-10) tend to exhibit higher stress concentrations at the corners which can accelerate defect propagation. In contrast, defects with rounded or smooth edges (rated 1-5) are more stable, as the applied forces are more evenly distributed, reducing the likelihood of further deterioration.

3.2 Collective Effect

Apart from the impact of individual defects mentioned in the previous section, the collective effect of multiple defects should also be investigated, as defects often occur in clusters. When multiple defects appear within a single structural unit, various factors, such as intensity influence and center influence, should all be considered. The combined effect of these factors is illustrated in Figure 2.

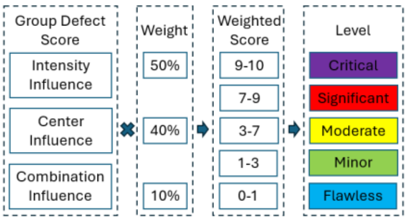

Figure 2. Proposed systematic workflow for group defect ranking of component.

3.2.1 Intensity Influence

Distance is the primary indicator of the combined impact of multiple defects. When defects are densely concentrated within a specific area, the local structural zone becomes more vulnerable, increasing the likelihood of sudden failure. Two approaches can be employed to quantify the level of defect concentration.

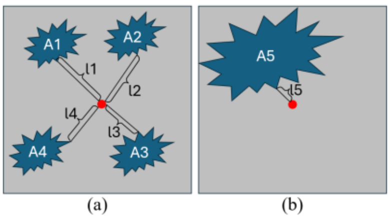

Figure 3. Combined impact factor: (a) adjusted weighted approach, and (b) finding the initial defect.

The first step involves calculating the adjusted weighted intensity factor (see Equation 3) based on a distance function, as illustrated in Figure 3 (a). In this equation, A_i represents the defect area, d_i denotes the distance between two defects, β is the scaling factor, and I_i is the intensity factor when a single defect is positioned at the center. Different initial defect locations may lead to varying results. Since this index is computed with respect to a single center, the outcome may be biased. To enhance scientific accuracy and minimize bias, the weighted intensity factor WI is introduced (see Equation 4). This factor is derived by averaging the individual intensity indices within the same structural component, as shown in Figure 3 (b).

$$I_i = \frac{\sum_1^i A_i e^{-\beta d_i}}{\sum_1^i A_i} \tag{3}$$

$$WI = \frac{\sum_1^i I_i}{i} \tag{4}$$

3.2.2 Center Influence

In addition to the influence of defect density, the group effect on the structural component itself should also be analyzed, as illustrated in Figure 4. In this figure, $A_1 - A_4$ represent defect areas, while $D_1 - D_4$ denote vectors extending from the geometric center of the structural component to the centers of individual defects. The red dot indicates the geometric center of the component.

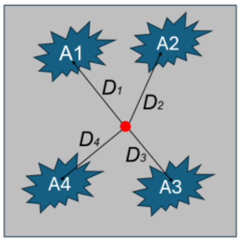

Figure 4. The center impact of the defects towards the center of the component.

The center impact of defects is a key parameter for evaluating their overall effect on a structural component. This index accounts for both the direction and distance of each defect relative to the component's geometric center. The magnitude of the resulting general vector represents the overall impact. The calculation of the center impact index is detailed in Equations 5-7, where k is the scale factor, A_i represents the defect area, D_i is the vector from the component center to defect center, W_i is the weighted vector, V_x is the influence vector in x direction, V_y is the influence vector in y direction, V_z is the influence vector in z direction, and V_i is the gross center influence vector.

$$W_i = D_i \cdot A_i \tag{5}$$

$$V_i = \frac{\sum_1^i k \cdot W_i}{\sum_1^i A_i} \tag{6}$$

$$|V_i| = \sqrt{{V_x}^2 + {V_y}^2 + {V_z}^2} \tag{7}$$

3.2.3 Combination Influence

When more than one kind of defect appears on the same component, combination factor is introduced to calculate the interaction effects between different types of defects. Different combinations of multiple defects can signify varying structural issues. For example, in the case of corrosion, cracking, and spalling, severity increases progressively from the infiltration of greenish deposits to cracks and then to a peeled concrete surface. The presence of both corrosion and cracks generally has a lower CF compared to the combination of cracks and spalling, which directly endangers structural integrity. If only one type of defect is involved in the component, CF is not applied and regarded as the minimum of 1.

4 Case Study

To evaluate the effectiveness of the proposed rating system, a case study is conducted on an aging cooling tower. The study begins with a brief introduction to the background of the cooling tower. High-resolution images were first captured by a UAV (see Figure 5), as well as LiDAR point cloud data using a terrestrial laser scanner (see Figure 6). Subsequently, a spalling BIM model (see Figure 7) is generated in Autodesk Revit using. Finally, a detailed analysis is performed based on the proposed methodology, utilizing the extracted spalling information to assess defect severity.

Figure 5. Captured image of spalling near the top ring of an aging cooling tower.

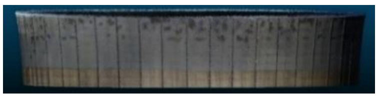

Figure 6. The captured LiDAR point clouds of defective area near the top ring of an aging cooling tower.

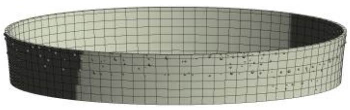

Figure 7. The BIM model of the aging cooling tower with spalling spread on the surface.

4.1 Project Background

Since the cooling tower became operational, high-temperature steam has condensed into moisture near the top ring, leading to the gradual corrosion of the concrete surface, as shown in Figure 5. After decades of cyclic exposure, the surface began to swell and eventually detach, resulting in concrete debris falling. These detached fragments pose a significant safety risk to workers on the ground. More critically, the exposure of reinforcement bars accelerates their deterioration, as continuous steam exposure enhances corrosion. Over time, this degradation may damage the stability of the upper structure. Therefore, monitoring the distribution of spalling and assessing its severity across different areas is important for ensuring structural integrity and worker safety.

4.2 Data Analysis

As outlined in Section 3, the individual effects are analyzed in the context of a specific case where spalling is the main defect, and the structure exhibits uniform properties. Additionally, the group effects, primarily including intensity influence and center influence, are quantified according to the conditions observed in the cooling tower. These calculations provide a comprehensive assessment of defect severity.

4.2.1 Individual Effect

The recorded spalling areas, measured in square meters, range from $0.03m^2$ to $4m^2$. These areas are categorized into three groups based on area: minor spalling ($0m^2$-$0.5m^2$), moderate spalling ($0.5m^2$-$1m^2$), and major spalling ($1m^2$-$4m^2$). In this case, a total of 157 minor defects, 54 moderate defects, and 25 major defects were identified. The severity scores assigned to these categories are 3 points for minor defects, 7 points for moderate defects, and 10 points for major defects.

The significance of location is primarily determined by its impact on load-bearing structures. In the case of the cooling tower, the entire structure is axisymmetric, meaning that all concrete panels serve an equivalent functional role. Consequently, height is the key variable influencing location-based importance. The height range is classified into three categories: minor effect (605m-608m), moderate effect (608m-612m), and major effect (612m-615m). Based on these criteria, 17 spalling locations are classified as non-critical (scoring 3 points), 85 locations are categorized as concerning (scoring 7 points), and 134 locations are identified as critical (scoring 10 points).

Regarding shape, no prominent spiky edges were observed among the existing spalling. Instead, most defects exhibit irregular forms. Some examples of these irregular and smooth-edged shapes are presented in Figure 8. Since the defects lack sharp edges, a severity score of 6 is assigned to irregularly shaped spalling, while round-shaped defects are given a lower severity score of 1.

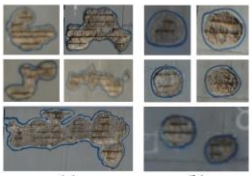

Figure 8. Two shapes of defects: (a) irregular/spiky shapes, and (b) smooth shapes.

As observed in Figure 5, the defects near the top ring primarily consist of spalling. Due to the lack of recorded data, the exact duration of defect existence remains unknown. Similarly, the exposure conditions are largely uniform because all defects are located on the concrete surface at similar heights. Therefore, the indexes for defect type, existing time, and exposure condition can be excluded from the analysis.

As discussed above, three main factors – spalling area, location, and shape are considered in the evaluation. The weighting of assessment criteria represents the relative impact of severity for each type of defect. The weights are determined based on practical inspection experience and engineering judgment in this study. Dimensions of defects are put in the first place as surface material loss is directly related to structural integrity. Location of defects is regarded as the second important factor as the appearance in critical areas can also pose significant safety risks to structural capacity. Shape of defect is allocated a lower weight because the influence is less compared to other two factors. Future studies will adopt more structured approaches or expert surveys to refine the scheme. The weight distribution for these factors is assigned as follows: 50% for area, 40% for location, and 10% for shape. The calculated factors for Panel 1 are provided as an example (see Table 1).

Table 1 Scaled area, location, and shape factors for Panel 1.

Spalling No.	1-1	1-2	1-3	1-4	1-5	1-6	1-7
Area Factor	10	3	3	7	3	7	7
Location Factor	10	10	10	10	10	7	7
Shape Factor	1	1	1	1	1	1	1
Scaled Area Factor	5	1.5	1.5	3.5	1.5	3.5	3.5
Scaled Location Factor	4	4	4	4	4	2.8	2.8
Scaled Shape Factor	0.1	0.1	0.1	0.1	0.1	0.1	0.1

4.2.2 Collective Effect

This section examines the impact caused by multiple defects, specifically focusing on intensity influence and center influence. Since only a single defect type is present, the combination factor is not considered. In this case, the structural unit used for calculating the group effect is a concrete panel. Take Panel 1 as an example, the centers of the identified spalling defects are marked in Figure 9 (a), while the geometric center of the panel is indicated in Figure 9 (b).

Figure 9. Panel 1: (a) numbered centers of spalling, and (b) the center of panel component.

Following Equation 3, the scaling factor β is set to 0.1. The intensity index for different spalling instances is presented in Table 2. As observed, variations in the spalling center result in changes in the intensity index, ranging from 0.7458 to 0.8599. To mitigate potential bias, the derived single intensity indexes are averaged according to Equation 5.

Table 2. Individual intensity factors for spalling on panel 1.

Spalling	Single Intensity Index
1-1	0.8599
1-2	0.7739
1-3	0.8028
1-4	0.8529
1-5	0.8101
1-6	0.7458
1-7	0.7808

For the center index, individual weighted vectors are calculated using Equation 5. Afterward, the scaling factor k is set to 0.2 to obtain the magnitude of the gross center influence index for each concrete panel, as calculated using Equation 6 and 7.

Since only spalling appears on the concrete surface, the combination factor is excluded from the analysis. The group effect factors are weighed as follows: 60% for the intensity influence index and 40% for the center influence index. The intensity influence, center influence index, and combined group effect factors for panel 1 to 10 are listed in Table 3.

Table 3. Calculated influence index for panels 1 to 10.

Panel	Intensity Influence Index	Center Influence Index	Combined Group Index
1	0.8037	0.7155	0.8
2	0.8060	0.8254	0.8
3	0.7568	0.5501	0.7
4	0.7509	0.4367	0.6
5	0.8303	0.4273	0.7
6	0.8111	0.4015	0.6
7	0.8037	0.3436	0.6
8	0.7808	0.5214	0.7
9	0.8368	0.6863	0.8
10	0.8181	0.6571	0.8

To validate the statistics derived, the distribution of spalling on each concrete panel is shown in Figure 10. As previously discussed, the more concentrated the spalling defects are in each area, the higher the value of the intensity influence index. For example, even with a similar amount of spalling, the intensity index of Panel 9 is higher than that of Panel 8 due to the more concentrated spalling in Panel 9. For the center influence index, the value increases as the spalling group moves farther away from the center of the panel. As seen from panel 25 to 27, the center influence index decreases as the defect groups move closer to the panel center.

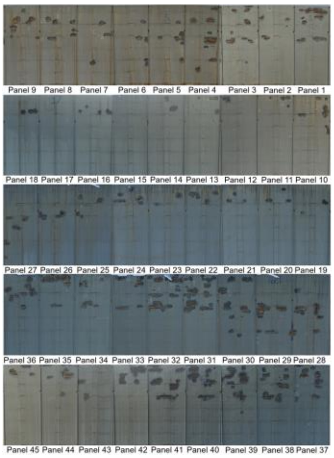

Figure 10. The projected top ring panels of defects.

4.3 Panel Defect Index

Since both the individual defect scores and group factors are available, the panel defect index can be determined. Figure 11 presents a comparison between the panel defect index obtained using the proposed methodology and the index based solely on the spalling area. The top 10 highest indexes are highlighted in red, the 10 lowest indexes in green, and the moderate values in yellow. The differences in severity rankings indicate that the proposed method offers a more comprehensive assessment by incorporating multiple defect-related factors.

Panel	Panel Defect Index	Pure Area Index	Panel	Panel Defect Index	Pure Area Index	Panel	Panel Defect Index	Pure Area Index
1	37.04	4.49	16	18.32	0.85	31	64.24	6.92
2	26.48	2.98	18	11.88	0.90	32	59.52	6.28
3	37.03	3.17	19	8.00	0.57	33	31.36	3.10
4	23.64	2.63	20	15.12	0.70	34	27.60	2.38
5	19.95	2.00	21	15.12	0.56	35	16.56	4.46
6	12.00	1.43	22	21.96	1.36	36	35.68	4.20
7	7.98	1.14	23	11.88	0.71	37	41.36	4.01
8	21.35	1.91	24	24.21	1.88	38	46.24	4.61
9	29.20	2.87	25	17.60	1.08	39	42.16	5.66
10	27.60	2.31	26	13.72	1.29	40	43.44	5.19
11	22.41	0.72	27	11.10	1.57	41	42.48	6.20
12	11.20	0.58	28	21.18	3.95	42	27.36	3.83
13	15.12	0.87	29	15.42	3.62	43	11.60	1.12
14	11.88	0.94	30	37.03	4.37	44	32.76	2.64
						45	18.72	1.76

Figure 11. Comparison between the panel defect index and sum of spalling area.

To better understand the distribution of defects, spalling is modeled into different sizes to indicate the affected area (see Figure 12 (a)). The colors represent varying severities, ranging from green (minor) to yellow (moderate) and red (severe). Additionally, the categorized concrete panels based on the defect index are presented in Figure 12 (b). A combined visualization of both the panels and spalling is displayed in Figure 12 (c) to provide a comprehensive overview of the structural condition.

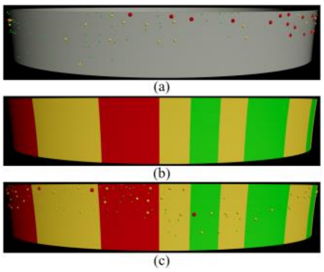

Figure 12. (a) The categorized spalling: green ($0m^2 - 0.5m^2$), yellow ($0.5m^2 - 1m^2$), and red ($1m^2 - 4m^2$), the categorized panel based on defect index: green (minor), yellow (moderate), and red (major), and (c) the categorized panel and spalling

4.4 Validation

The proposed framework is evaluated through comparative analysis and engineering consistency assessment. Compared with the conventional area-based approach, the proposed method derives a more comprehensive result by considering multiple attributes. The assessment is also consistent with engineering deductions, when higher concentration and more critical location can lead to higher scores. Future work is expected to perform a direct comparison with expert assessments.

5 Discussion

The proposed methodology is applied to an aging cooling tower to demonstrate its feasibility. A semantically rich defect specification model is developed, incorporating essential defect and component rating information. To enhance interpretability, the severity of defects is visualized using a color-coded system, facilitating intuitive assessment of structural conditions. This enhanced visualization supports decision-making and maintenance strategy development by leveraging the defect BIM model and parameterized information. The proposed rating system is designed to be adaptable across different projects. Although certain criteria involve limited engineering judgement, explicit scoring rules can maintain repeatability and consistency. One of the main challenges remains the absence of common standards for validating results which can affect the reliability of evaluations. Future research will focus on standardizing the assessment criteria to improve the consistency and robustness of the defect rating system. The integration of Knowledge Graph (KG) could facilitate a more thorough understanding of defect propagation and interdependence.

6 Conclusions

The increasing number of aging infrastructure assets can potentially pose dangers to structural safety and human users. To mitigate the bias introduced by traditional human-based inspections, this study presents a practical workflow - from rating the condition of defects to visualizing categorized defects within a BIM model. A comprehensive assessment criterion is proposed, considering both individual and grouped defect effects. The individual defect assessment includes factors such as type, location, dimension, exposure condition, existing time, and shape. Each factor is assigned a score based on its severity. By multiplying the weights of these factors and summing the scaled values, the overall score for individual defect can be calculated. This score is then aggregated at the component level. Next, group factors – including intensity, center, and combination influences - are evaluated. Integrating both individual and group factors provides a more reasonable defect score for each component.

Acknowledgments

This research is supported by funding from the Australian Research Council (ARC) Research Hub for Resilient and Intelligent Infrastructure Systems (IH210100048), and the ARC Research Hub for Human-Robot Teaming for Sustainable and Resilient Construction (IH240100016).

References

[1] P. Borin and F. Cavazzini. Condition assessment of RC bridges: Integrating machine learning, photogrammetry and BIM. *The International Archives of the Photogrammetry, Remote Sensing and Spatial Information Sciences*, 42:201–208, 2019.

[2] I. S. Dias, I. Flores-Colen, and A. Silva. Critical analysis about emerging technologies for building's façade inspection. *Buildings*, 11(2):53, 2021.

[3] N. Bolourian. *Point cloud-based deep learning and UAV path planning for surface defect detection of concrete bridges*. Concordia University, 2022.

[4] Y. Guo, Z. Wang, X. Shen, K. Barati, and J. Linke. Automatic detection and dimensional measurement of minor concrete cracks with convolutional neural network. *ISPRS Annals of the Photogrammetry, Remote Sensing and Spatial Information Sciences*, 10:57–64, 2022.

[5] Y. Guo, X. Shen, J. Linke, Z. Wang, and K. Barati. Quantification of structural defects using pixel level spatial information from photogrammetry. *Sensors*, 23(13):5878, 2023.

[6] M. Choi, S. Kim, and S. Kim. Semi-automated visualization method for visual inspection of buildings on BIM using 3D point cloud. *Journal of Building Engineering*, 81:108017, 2024.

[7] A. Y. Yiğit and M. Uysal. Automatic crack detection and structural inspection of cultural heritage buildings using UAV photogrammetry and digital twin technology. *Journal of Building Engineering*:109952, 2024.

[8] F. Bahreini and A. Hammad. Developing an ontology for concrete surface defects to enhance inspection, diagnosis and repair information modeling. *Infrastructures*, 9(12):220, 2024.

[9] D. Uzarski. *Development of condition indexes for low volume railroad track*. 1993.

[10] N. Amani, M. Nasly, and R. A. Samat. Infrastructure component assessment using the condition index system: Literature review and discussion. *Journal of Construction Engineering and Project Management*, 2(1):27–34, 2012.

[11] Queensland Government. *Structures inspection manual*. Structures inspection manual. On-line: https://www.tmr.qld.gov.au/_/media/7c6ed28706904a0fb9664bddccc01fc2.pdf, Accessed: 31/12/2025.

[12] VicRoads. *Bridge maintenance and repair manual*. Bridge maintenance and repair manual. On-line: https://content.vic.gov.au/sites/default/files/2024-05/Bridge-Maintenance-and-Repair-Manual-%28v1.5%29.pdf, Accessed: 31/12/2025.